Testicular degeneration in *Bclw*-deficient mice

Andrea J. Ross[1], Katrina G. Waymire[1], Julie E. Moss[2], A.F. Parlow[3], Michael K. Skinner[4], Lonnie D. Russell[5] & Grant R. MacGregor[1]

To identify genes required for mammalian spermatogenesis, we screened lines of mutant mice created using a retroviral gene-trap system[1] for male infertility. Homozygous ROSA41 male mice exhibit sterility associated with progressive testicular degeneration. Germ-cell defects are first observed at 19 days post-natal (p19). Spermatogenesis is blocked during late spermiogenesis in young adults. Gradual depletion of all stages of germ cells results in a Sertoli-cell-only phenotype by approximately six months of age. Subsequently, almost all Sertoli cells are lost from the seminiferous tubules and the Leydig cell population is reduced. Molecular analysis indicates that the gene mutated is *Bclw*, a death-protecting member of the *Bcl2* family. The mutant allele of *Bclw* in ROSA41 does not produce a Bclw polypeptide. Expression of *Bclw* in the testis appears to be restricted to elongating spermatids and Sertoli cells. Potential roles for *Bclw* in testicular function are discussed.

The ROSA41 mouse strain was generated using the ROSA β-gal retroviral gene trap[1]; heterozygotes were phenotypically indistinguishable from wild-type mice. Genotype analysis of offspring from heterozygous inter-crosses (87 +/+ : 154 +/− : 78 −/−) suggested that no lethality is associated with homozygosity for the proviral insert. Homozygous mutant ROSA41 mice weighed less than their heterozygous or wild-type litter mates [average weight 83.8% of control litter-mates; range 66.3–99.6%; n=11 (+/+), 32 (+/−), 26 (−/−)]. Although homozygous ROSA41 mutants were usually smaller at birth, their growth curves were indistinguishable from control animals suggesting that the defect arises prenatally (data not shown). Homozygous mutant ROSA41 males

were sterile, with no defects observed in the external genitalia of homozygous mutants; testicular descent appeared normal. The testes and seminal vesicles of homozygous mutant males, however, were reduced in size compared with controls (Fig. 1a). Seminal-vesicle weight in homozygous mutants decreased with increasing age, the values ranging from 100% of controls at 5 months of age to less than 10% at 14 months. Plasma levels of follicle-stimulating hormone (FSH) were significantly increased in homozygous mutants at all ages analysed between 2.5 and 15 months of age [2.05-fold, s.e.m. 0.35; n=3 (+/+), 9 (+/−), 7 (−/−), $P<0.05$]. No consistent difference was observed in luteinizing hormone (LH) levels (data not shown) and no other gross organ hypoplasia or hyperplasia was observed in homozygous ROSA41 mice.

The gene mutated in the ROSA41 line of mice was identified by cloning and sequencing genomic DNA flanking the single proviral integration site. Comparison of genomic DNA sequence flanking the provirus to databases suggested that the gene mutated by the proviral insertion was *Bclw*[2], a death-protecting member of the *Bcl2* gene family (Fig. 1b). The provirus integrated 134 bp upstream of exon 3 (Fig. 1c). 5′ RACE (ref. 3) was used to identify 120 bp of sequence of the transcript trapped by the ROSA β-gal provirus. To confirm that the RACE product represented the 5′-untranslated region of *Bclw* mRNA, a mouse-brain cDNA-library was screened with this product and two independent clones sequenced (data not shown). Results confirmed that *Bclw* was trapped by ROSA β-gal in the ROSA41 line. The mutant allele has been named *Bclw^Gtrosa41*. RT-PCR and western analysis were used to screen for transcripts capable of
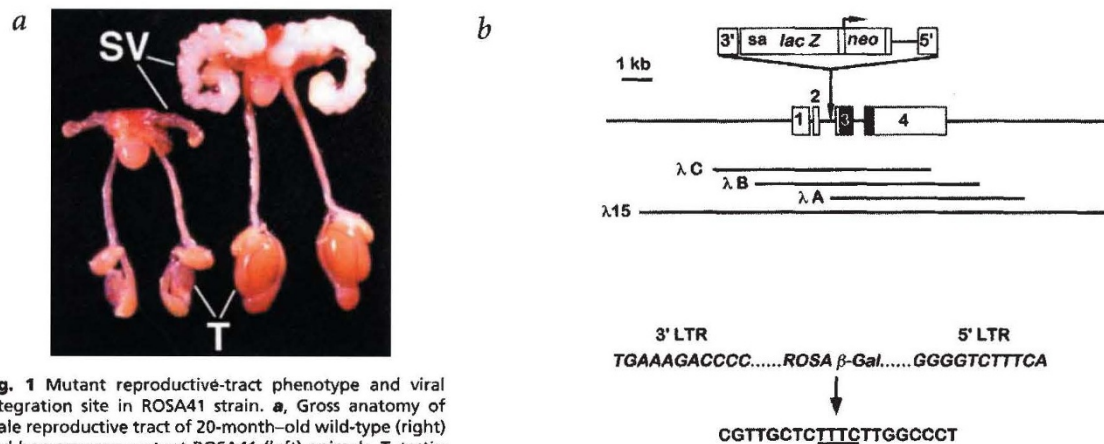

Fig. 1 Mutant reproductive-tract phenotype and viral integration site in ROSA41 strain. *a*, Gross anatomy of male reproductive tract of 20-month–old wild-type (right) and homozygous mutant ROSA41 (left) animals. T, testis; SV, seminal vesicle. *b*, Integration of the ROSA β-gal provirus within the *Bclw* locus in the ROSA41 line of mice. *Bclw* exons are depicted by numbered boxes. The coding sequence is indicated in black. Genomic-DNA inserts from three independent lambda clones containing the proviral integration (λA–C) or wild-type (pre-integration) site (λ15) are indicated below. *c*, Sequence of proviral integration site within intron 2 of *Bclw*. From top to bottom are the sequence of the inverted repeats at the ends of the provirus (italics), the wild-type pre-integration site and the junction sequences of the integrated provirus. The 4-bp target site that was duplicated during retroviral integration is underlined.

[1]*Center for Molecular Medicine, Emory University School of Medicine, 1462 Clifton Rd. NE, Atlanta, Georgia 30322, USA.* [2]*BBSRC Center for Genome Research, University of Edinburgh, Kings Buildings, Edinburgh EH9 3JQ, UK.* [3]*Harbor-UCLA Medical Center, 1000 West Carson Street, Torrance, California 90509, USA.* [4]*Center for Reproductive Biology, Department of Genetics and Cell Biology, Washington State University, Pullman, Washington 99164, USA.* [5]*Dept. of Physiology, Southern Illinois University School of Medicine, Carbondale, Illinois 62901, USA. Correspondence should be addressed to G.R.M. e-mail: gmacg@bimcore.emory.edu*

Fig. 2 Bclw expression in ROSA41 animals. **a**, RT-PCR analysis of Bclw mRNA in mutant and control ROSA41 mouse tissues. The cartoon depicts the location of the primers used in the RT-PCR assay and the size of amplification products derived from genomic DNA or cDNA. **b**, RT-PCR analysis of Bclw using RNA isolated from testis (T), brain (B) or salivary gland (SG) of wild-type or homozygous mutant animals (upper band). Control PCR amplification of Hprt cDNA using same template in the lane immediately above (lower band). The only signal observed in the reactions using RNA from ROSA41 homozygotes is derived from contaminating genomic DNA. **c**, Western analysis of total protein from transfected COS cells, freshly isolated mouse Sertoli cells, and from wild-type and homozygous-mutant ROSA41 brains and testes. Lane 1, COS-7 cells transfected with pCMV expression vector[21] without a cDNA insert; Lane 2, COS-7 cells transfected with a pCMV-Bclw cDNA; Lane 3, freshly isolated p18 mouse Sertoli cells; Lane 4, wild-type ROSA41 testis; Lane 5, homozygous-mutant ROSA41 testis; Lane 6, wild-type ROSA41 brain; Lane 7, homozygous-mutant ROSA41 brain. The size of Bclw peptide (22 kD) is indicated by the arrowhead. The antisera also crossreacts with peptide(s) of approximately 18 kD that are found in (monkey) COS cells and mouse testis and at lower levels in mouse brain.

encoding Bclw in tissues from ROSA41 homozygote mutants. No transcript containing the Bclw coding sequence could be detected in brain, salivary gland or testis of homozygous ROSA41 mutant animals (Fig. 2a,b). Similarly, western analysis demonstrated an absence of Bclw in the brain and testis of homozygous ROSA41 mice (Fig. 2c). Thus, the $Bclw^{Gtrosa41}$ allele does not appear to produce a mRNA that can encode Bclw.

As the $Bclw^{Gtrosa41}$ transcript encodes lac Z (β-galactosidase), X-gal staining of heterozygous ROSA41 testes was used to identify the testicular cells that express $Bclw^{Gtrosa41}$ (Fig. 3a–d). Sectioning of seminiferous tubules revealed that $Bclw^{Gtrosa41}$ is expressed in
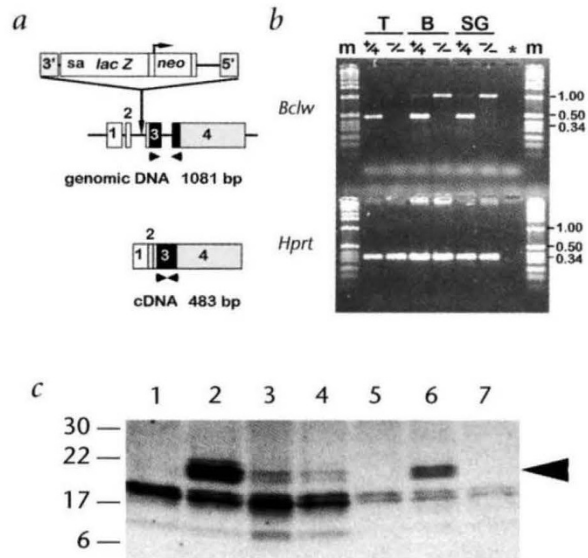
elongating spermatids between steps 11 and 16 (Fig. 3a,c, and data not shown). Significantly weaker expression was also observed in Sertoli cells although not all Sertoli cells stained blue (Fig. 3b,d). No consistent staining was observed in other testicular cells, despite prolonged incubation with X-gal. To determine whether the X-gal staining reflected the cells in which Bclw is expressed, immunohistochemistry (IHC) was performed using testes from wild-type and homozygous mutant ROSA41 animals (Fig. 3e–h). Bclw protein could first be detected over the nucleus and cytoplasm of step-10 spermatids (Fig. 3f). By step 16, most of the protein appeared to be localized to the residual body (Fig. 3g). No staining was observed in elongating spermatids in homozygous mutant ROSA41 testes (Fig. 3h). Although Bclw protein could not be detected in Sertoli cells using IHC, western analysis of Sertoli cells isolated from p18 wild-type male mice confirmed that Bclw is present in mouse Sertoli cells (Fig. 2c). Thus, good agreement was observed between testicular expression of $Bclw^{Gtrosa41}$ and presence of Bclw protein.

Testis histology was examined from homozygous mutant and wild-type ROSA41 males between p16 and 8 months of age (Figs 4–6). Periodic acid-Schiff's (PAS)-haematoxylin staining was used to examine cytology and identify degenerating germ cells, and anti-GCNA antibody[4] was used to detect spermatogonia; TUNEL or electron microscopy was used to detect cells
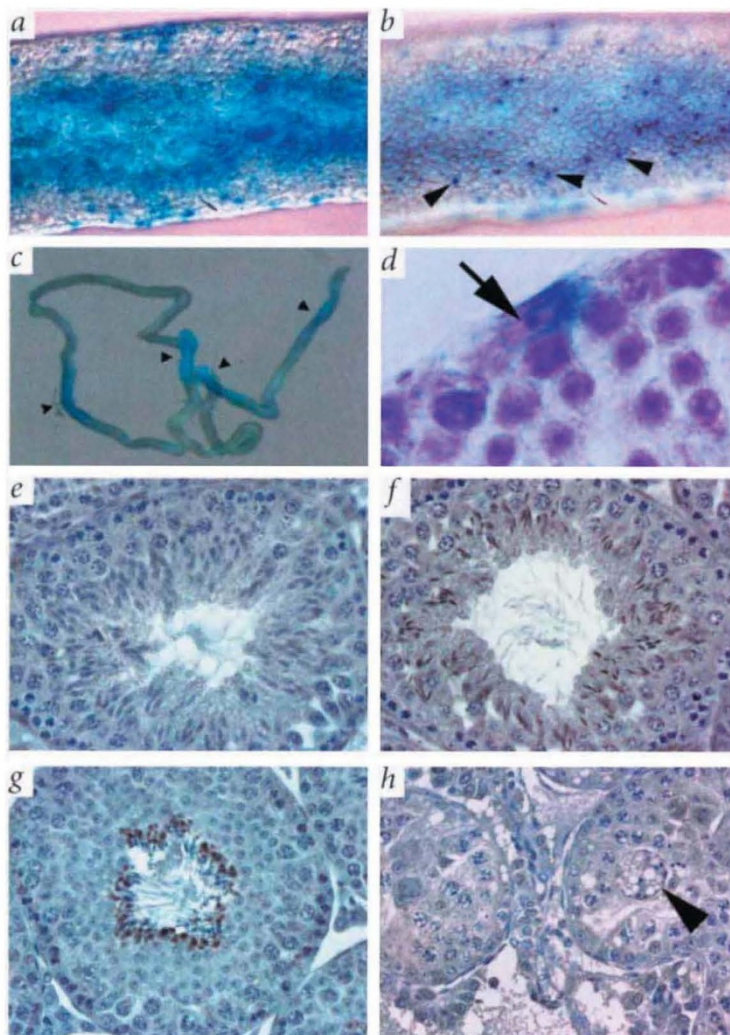
Fig. 3 Expression pattern of Bclw in testis. **a**, Whole-mount of a seminiferous tubule from an adult heterozygous ROSA41 animal fixed and stained with X-gal for β-gal activity. Staining can be observed within the elongating spermatids in the lumen in addition to cells in the periphery of the tubule. **b**, Same tubule, focused to show staining within the basement-membrane region of the tubule (arrowheads). **c**, Low-magnification view of whole tubule showing spatially periodic expression of $Bclw^{Gtrosa41}$ due to presence in elongating spermatids (arrowheads). **d**, High-magnification view showing example of β-gal activity surrounding a Sertoli-cell nucleus (arrow). **e**, IHC of wild-type seminiferous epithelium containing step-9 spermatids from 2.5-month–old animal. No staining is evident within the spermatids. **f**, Step-10 spermatids with staining predominantly over the nucleus. **g**, Stage-VIII tubule containing step-16 spermatids with Bclw protein in residual bodies. **h**, IHC using 2.5-month–old homozygous testis. No staining is observed within the symplast of degenerating elongate spermatids in the right tubule (arrowhead). Tissues were fixed and processed simultaneously under identical conditions.

Fig. 4 Development of early mutant phenotype in homozygous mutant ROSA41 testis. ***a–c***, p24 wild-type. ***d–f***, p24 ROSA41 homozygous mutant. ***g–i***, 2.5-month–old wild-type. ***j–l***, 2.5-month–old homozygous mutant. ***m–o***, 6-month–old homozygous mutant. The stains used are PAS and haematoxylin (left column), anti-GCNA immunohistochemistry - haematoxylin (middle column) and TUNEL (right column). Magnification: ×200.
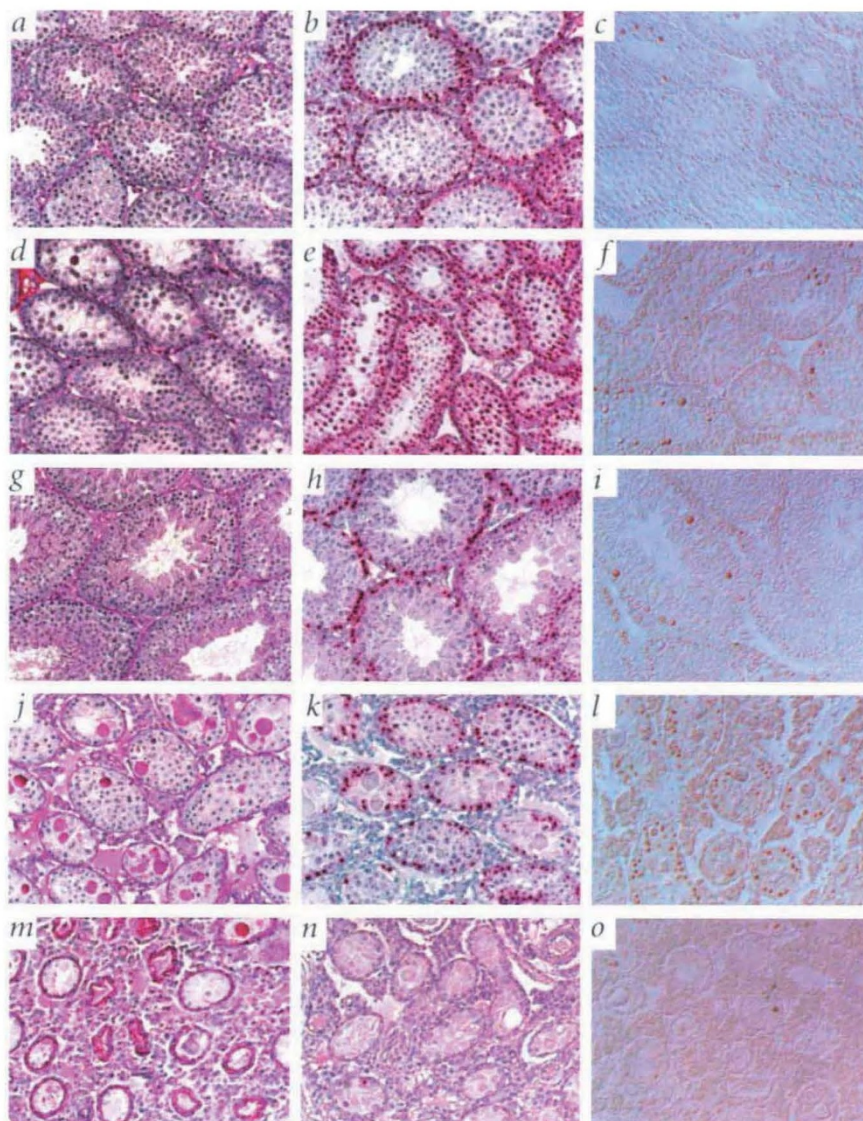

undergoing apoptosis. At p16, no significant difference was observed in either absolute numbers or the ratio of spermatogonia and spermatocytes in homozygous mutant and control ROSA41 mice (data not shown). In addition, no difference was observed in numbers of degenerating germ cells. While wild-type and mutant p19 testes contained similar numbers of germ cells, the incidence of degenerating spermatocytes was increased seven fold in mutants (data not shown). In mutants at p24 (Fig. 4*d*), there was a ten fold reduction in spermatid number compared with control testes (Fig. 4*a*). The number of degenerating germ cells was also increased, including cells undergoing apoptosis (Fig. 4*f*), and the mutant seminiferous epithelium was disorganized with poor lumen formation (Fig. 4*d*). The majority of TUNEL-positive cells in mutant testes at this stage were spermatocytes. Testes cytology in p32 homozygous mutants and control littermates was examined by electron microscopy. Elongating spermatids undergoing nuclear condensation were observed in control testes (Fig. 5*a*). In contrast, all elongating germ cells in homozygous ROSA41 testes displayed extensive cytoplasmic vacuolation, suggestive of cellular degeneration (Fig. 5*b*). No elongating spermatids more advanced than step 13 were observed in the testes nor were spermatozoa observed in the epididymides of homozygous mutant males. All stages of developing germ cells were found in 2.5-month adult control testes (Fig. 4*g*). There was an absence, however, of mature spermatids in testes from mutant littermates (Fig. 4*j*). In addition, the seminiferous epithelium was highly disorganized and the majority of tubules contained PAS-staining material without evidence for nuclear structures. Large numbers of germ cells underwent apoptosis at this time as shown by both TUNEL staining (Fig. 4*l*) and electron microscopy (Fig. 5*d*). Anti-GCNA staining (Fig. 4*k*) confirmed that there were fewer spermatogonia compared with control testis (Fig. 4*h*). By approximately 6 months of age, most seminiferous tubules of ROSA41 homozygotes lacked germ cells (Fig. 4*m,n*), which was the reason for the reduction in TUNEL-positive nuclei (Fig. 4*o*). We found no evidence for apoptosis-mediated death of Sertoli cells by either TUNEL (Fig. 4*o*) or electron microscopy (Fig. 5*e*). To determine if germ-cell loss was associated with increased rate of spermatogonial proliferation, we compared the mitotic index of spermatogonia in mutant and control testes using an antibody against PCNA (ref. 5). We observed no significant difference on comparing homozygous-mutant and control testes between p16 and 2.5 months of age (data not shown).

While many germ cells were found in 2.5-month–old ROSA41 homozygotes (Fig. 6*a,b*), most were lost in the 5-month–old animal (Fig. 6*c,d*). Despite shrinkage of the seminiferous tubules, there were areas within the lymphatic space that appeared to reflect localized hyperplasia of Leydig cells (Fig. 6*c*; lower aspect). By 6.5 months of age (Fig. 6*e,f*), germ cells were rare and Leydig-cell loss was observed. Remaining Leydig cells were often clustered around the tubules and blood vessels (Fig. 6*f*). At 8 months (Fig. 6*g,h*), most Sertoli cells were sloughed or lost from the tubules (Fig. 5*f*). There was also a significant reduction in numbers of Leydig cells. Peritubular-myoid, endothelial-cell and extracellular–matrix (ECM) layers, however, appeared to remain intact.

Mammalian spermatogenesis requires intricate regulation of cell proliferation, differentiation and apoptosis. The Sertoli cell is the somatic component of the seminiferous epithelium that supports maintenance and development of germ cells[6]. Increased numbers of spermatogonia undergo apoptosis between p8 and p22 during normal mouse pre-pubertal development[7]. This may regulate the ratio of germ cells to Sertoli cells, thereby ensuring that adult Sertoli cell function is not compromised by excessive germ cells[8]. Genetic analyses have indicated that this process can be controlled by the Bcl2 pathway[9]. Expression of *Bcl2* within spermatogonia[10] or loss of function of the death-promoting Bcl2-family member, Bax[11], result in hyperplasia within the spermatogonial compartment with subsequent disruption of spermatogenesis. In neither case, however,

Fig. 5 EM analysis of testes from homozygous-mutant ROSA41 males. Elongate and round spermatids from wild-type (**a**) and homozygous (**b**) p32 ROSA41 testes. Condensing nuclei with attached flagella are observed in the wild-type histology. In the homozygous mutant, the nuclei condense but there is extensive vacuolation within the cytoplasm (asterisks). 2.5-month–old wild-type (**c**) and homozygous (**d**) ROSA41 seminiferous epithelia. The basal compartment of each tubule is shown. Chromatin condensation characteristic of cells in early stages of apoptosis is observed within the spermatogonia in the mutant testis (arrowheads). A germ cell in a more advanced state of apoptosis that has been engulfed by a Sertoli cell is also indicated (arrow). Homozygous testis histology at approximately 6 months (**e**) and 7 months (**f**) of age. The 6-month–old example illustrates a Sertoli-cell nucleus in advanced stages of decay (arrow). The basal membrane between the Sertoli cells and PMC (m) is marked by black arrowheads. In the 7-month–old sample, Sertoli cells are absent with the basal membrane (arrowhead) now defining the margin of the tubule lumen (asterisk); e, endothelial cell.
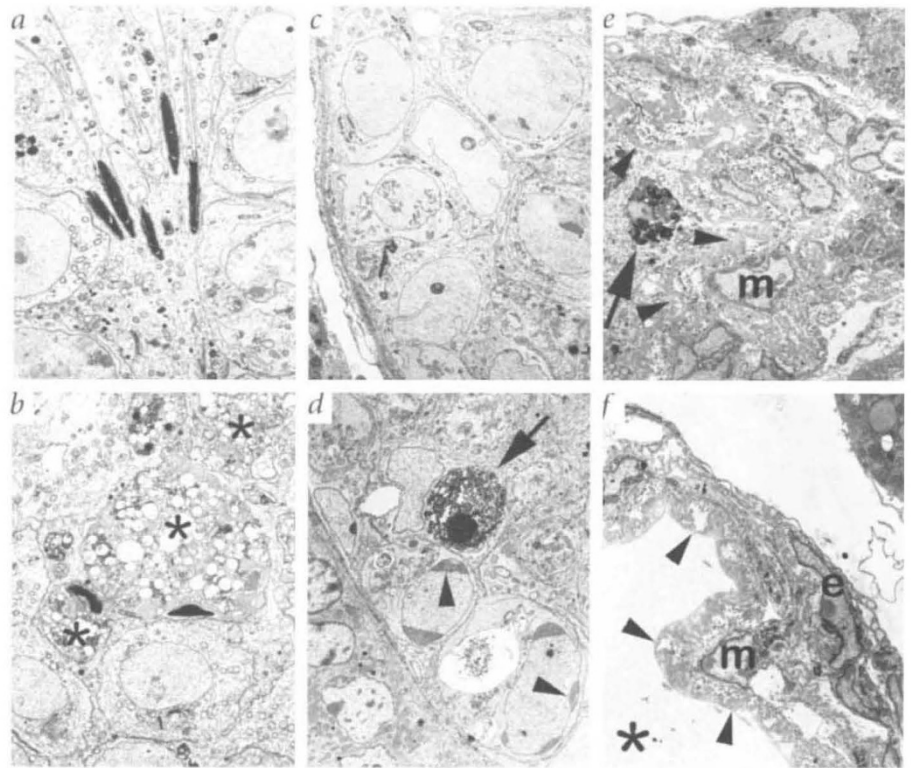
is extensive Sertoli-cell loss observed. Despite widespread expression in adult tissues[2], essential functions of *Bclw* appear to be restricted to the testis. It is possible that loss of *Bclw* function in other tissues is compensated by additional death-protecting *Bcl2* family members.

No firm conclusions can currently be drawn concerning the mechanism underlying testicular degeneration in *Bclw*-deficient mice. *Bclw* is expressed in wild-type elongating spermatids during the developmental stage at which *Bclw*-deficient germ cells arrest. Thus, *Bclw* may be required for haploid germ-cell differentiation in a cell-intrinsic manner. We cannot exclude the possibility that pre-meiotic germ-cell defects may be cell-intrinsic, involving loss of *Bclw* expression that is below the threshold detectable by IHC or X-gal staining of *Bclw*[Gtrosa41] heterozygotes.
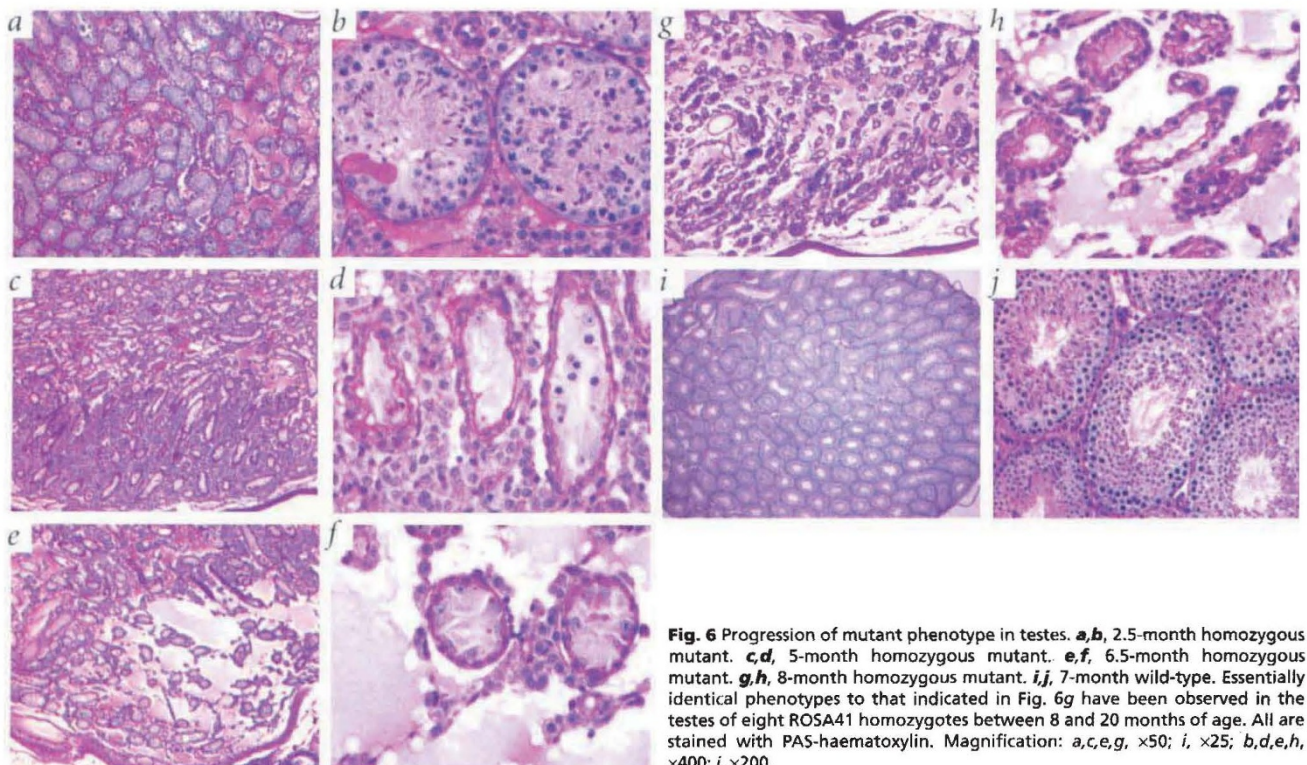

Fig. 6 Progression of mutant phenotype in testes. **a,b**, 2.5-month homozygous mutant. **c,d**, 5-month homozygous mutant. **e,f**, 6.5-month homozygous mutant. **g,h**, 8-month homozygous mutant. **i,j**, 7-month wild-type. Essentially identical phenotypes to that indicated in Fig. 6g have been observed in the testes of eight ROSA41 homozygotes between 8 and 20 months of age. All are stained with PAS-haematoxylin. Magnification: a,c,e,g, ×50; i, ×25; b,d,e,h, ×400; j, ×200.

Alternatively, the germ-cell defects may be an indirect effect of aberrant Sertoli cell function. Sertoli cells become post-mitotic at onset of puberty (approximately p17 in rodents[12]). Male germ-cell defects in *Bclw*-deficient mice are first observed in spermatocytes at p19. Thus, *Bclw* may be required for post-mitotic Sertoli cell function with loss of *Bclw* first being reflected in the delayed development and increased number of degenerating germ cells in pubertal animals. At least one death-promoting *Bcl2* family member, *Bak*[13], is expressed in mouse Sertoli cells (A.J.R. and G.R.M., unpublished observations). Loss of Bclw in Sertoli cells could potentially affect this cell type through an imbalance in levels of free Bak or other death-promoting Bcl2 family members.

If *Bclw* is indeed required in a cell-intrinsic manner for Sertoli cell survival, why do Sertoli cells persist in the absence of *Bclw* for up to six months? *Bclw*-deficient Sertoli cells may be sustained through interactions with germ cells. Sertoli cells express receptors for insulin-like growth factor-I (IGF-I) and nerve growth factor (NGF; ref. 14) which have the capacity to suppress apoptosis[15,16]. Germ cells are known to express both IGF-I (ref. 17) and NGF[18]. Production of these or other factors by germ cells could support survival of *Bclw*-deficient Sertoli cells but those cells in turn appear unable to support long-term survival of germ cells. Loss of germ cells would remove factor(s) without which the mutant Sertoli cells cannot survive. This model predicts that Sertoli-cell loss would occur significantly earlier in *Bclw* mutants that lack germ cells from birth. Adhesion of Sertoli cells to ECM can block apoptosis *in vitro*[19]. The lack of apoptotic features in *Bclw*-deficient Sertoli cells may be a consequence of Sertoli-ECM interactions. Finally, loss of Sertoli cells may remove paracrine signals[20] that sustain Leydig cells, which could account for the decrease within the Leydig-cell population and the reduced seminal-vesicle weight observed in the *Bclw* mutants over six months of age. Further analysis of *Bclw*-deficient mice will resolve the cell-autonomous nature of the reported defects and should provide novel insight into the role of *Bcl2*-family members in regulation of testis homeostasis.

Note in proof: The nomeclature of the mouse *Bcl2* family members is currently under consideration by the mouse nomenclature committee; the gene symbols are provisional.

Methods

Mice. The ROSA41 line was generated using the ROSA β-gal gene-trap virus as described[1]. The proviral integration site was given the locus assignment *Gtrosa41* and the *Bclw* allele was named *Bclw^Gtrosa41^*. All animal work was conducted using a protocol approved by the Emory University IACUC.

General molecular biology. The site of integration of the single ROSA provirus was cloned by constructing a genomic DNA library in λ DASH II (Stratagene) with homozygous ROSA41 DNA by conventional methods[22]. The retroviral pre-integration site was cloned from a similarly constructed 129/Sv-strain genomic library. Genomic DNA was subcloned into pBluescript (Stratagene) and inserts sequenced. All inserts were sequenced at least twice with ambiguities being resolved by sequencing the opposite strand. Sequence information was used to design a three primer/two allele PCR-genotyping assay. 5′ RACE (ref. 3) using total RNA isolated from testis was used to obtain sequence information of the trapped gene. The sequence was used to screen a brain cDNA-library constructed from a three-week-old C57BL10-strain mouse. Complimentary DNA clones were sequenced and compared to the 129/Sv genomic sequence to identify polymorphisms and to determine the exon–intron boundaries.

RT-PCR. Poly A$^+$ mRNA (1 μg) was reverse-transcribed in a 20-μl volume using random nonamer primers, 0.5 U RNAGuard (0.5 U; Pharmacia) and Superscript II MoMLV reverse transcriptase (RT; 20 U; BRL) in a buffer (supplied by BRL) under the following conditions: in a thermal cycler, the template was denatured at 95 °C for 2 min, followed by 30 °C during addition of RT with immediate ramping to 48 °C for 60 min, 60 °C for 5 minutes and 95 °C for 10 min to inactivate RT. Two percent of each cDNA reaction was used in a PCR containing each primer (166 nM), dNTP's (250 nM) and AmpliTaq (2.5 U; Perkin-Elmer) with 35 cycles of 95 °C, 1 min; 58 °C, 20 sec. The *Hprt*-PCR was effective in AmpliTaq buffer but the *Bclw*-PCR required addition of TaqExtender (2.5 U; Stratagene) and was conducted in TaqExtender buffer. Primers were: *Hprt*, 5′–CCTGCTG-GATTACATTAAAGCACTG–3′ (forward) and GTCAAGGGCATATC-CAACAACAAAC 5′–GTCAAGGGCATATCCAACAACAAAC–3′(reverse); *Bclw*: 5′–TTGCTGACTTTGTAGGCTATAAGC–3′ (exon 3, forward) and 5′–TCAGCACTGTCCTCACTGATGCCC–3′ (exon 4, reverse).

Mapping. Mapping was facilitated using a *Bam*HI-RFLP between C57BL/6J (9 kb) and *M. spretus* (4.5 kb) detected by a 2.3-kb *Eco*RI fragment within the *Bclw* gene. The Jackson Laboratory interspecific backcross panel (C57BL/6JEi×SPRET/Ei)F1×SPRET/Ei (Jackson BSS) was used as described[23]. Over 2700 loci that are evenly distributed among autosomes and the X chromosome have been mapped on this panel. Raw data are available at the URL http://www.jax.org/resources/documents/cmdata.

Serum gonadotropin level estimations. Male mice were caged singly for two weeks prior to serum isolation. Radio immuno-assays for FSH and LH in mouse serum were performed in duplicate using reagents distributed by the NIDDK's National Hormone and Pituitary Program including mouse FSH (AFP11454B) and LH (AFP5306A) antigen for iodination and NIDDK-anti rFSH-11 (1:62,500) and NIDDK-anti rLH-S-11 (1:750,000) antisera.

Antibody production and western analysis. Bclw-specific antisera was raised in rabbits following immunization with two peptides conjugated to KLH; MATPASTPDTRALVC-amide (amino acids 1–14) and Acetyl-DGALEEARRLREGNC-amide (amino acids 153–166; QCB, Inc.). Antibodies were affinity-purified by column chromatography using peptide coupled to activated Sepharose as described[22]. Sertoli cells were isolated from p18 male mice as described[24]. The purity of the Sertoli-cell preparation was estimated by microscopic examination to contain greater than 95% Sertoli cells, 3% peritubular myoid cells and no germ cells. For western analysis, tissues were solubilized in 150 mM NaCl, 10 mM EDTA, 50 mM TRIS (pH 7.6), 1% Triton-X100, 1% Na Deoxycholate containing leupeptin (1 μg/ml), aprotinin (3 μg/ml) and Pefabloc (500 μM; BMB) by homogenization followed by sonication. Total protein (40 μg) was electrophoresed through a NuPage gel (14%; NOVEX). Following electroblotting to nitrocellulose, the transfer efficiency was determined by staining in Ponceau S (0.1%). Membranes were blocked overnight, reacted with antibody, washed and signal was detected using a horseradish-peroxidase–conjugated secondary antibody (Donkey anti-rabbit, Amersham) in conjunction with ECL (Amersham). The N- and C-terminus–specific antibodies produced essentially identical results (data not shown).

Histology. Testes to be stained by PAS, TUNEL, PCNA and GCNA IHC were immersed overnight at 4 °C in Bouin's fixative. X-gal staining was performed on paraformaldehyde-fixed material as described[25]. For histology, tissues were cleared, infiltrated and embedded in paraffin wax and sections cut between 5 and 10 μm. Spermatogonia were detected using a germ-cell nuclear-antigen (GCNA)–specific antibody[4] in conjunction with an ABC kit (VectaStain Elite, Vector Labs). Degenerating germ cells were identified by their condensed nuclear staining and PAS-positive appearance. Apoptotic cells were detected by TUNEL using the InSitu Cell Death kit (BMB) as described by the manufacturer.

Electron Microscopy. Testes were perfused with gluteraldehyde by the vascular route[26]. Perfused testes were sectioned transversely by hand with a razor blade to obtain cross-sections of the seminiferous tubules. Following processing[27], tissue blocks were dehydrated, infiltrated and embedded in epoxy resin. Sections (approximately 1 μm) were stained with toluidine blue (1%) and examined by light microscopy to determine which blocks were to be thin-sectioned and subsequently examined by electron microscopy.

GenBank Accession Number. *Bclw*, AF030769.

1. Friedrich, G. & Soriano, P. Promoter traps in embryonic stem cells: a genetic screen to identify and mutate developmental genes in mice. *Genes Dev.* **5**, 1513–1523 (1991).
2. Gibson, L. *et al.* bcl-w, a novel member of the bcl-2 family, promotes cell survival. *Oncogene* **13**, 665–675 (1996).
3. Townley, D.J., Avery, B.J., Rosen, B. & Skarnes, W.C. Rapid sequence analysis of gene trap integrations to generate a resource of insertional mutations in mice. *Genome Res.* **7**, 293–298 (1997).
4. Enders, G.C. & May, J.J. Developmentally regulated expression of a mouse germ cell nuclear antigen examined from embryonic day 11 to adult in male and female. *Dev. Biol.* **163**, 331–340 (1994).
5. Hall, P.A. *et al.* Proliferating cell nuclear antigen (PCNA) immunolocalization in paraffin sections : an index of cell proliferation with evidence of deregulated expression in some neoplasms. *J. Pathol.* **162**, 285–294 (1990).
6. Russell, L.D. & Griswold, M.D. *The Sertoli Cell*. (Cache River Press, Clearwater, Florida, 1993).
7. Mori, C. *et al.* Morphological analysis of germ cell apoptosis during postnatal testis development in normal and Hsp 70-2 knockout mice. *Dev. Dynamic.* **208**, 125–136 (1997).
8. Huckins, C. The morphology and kinetics of spermatogonial degeneration in normal adult rats : An analysis using a simplified classification of germinal epithelium. *Anat. Rec.* **190**, 905–926 (1978).
9. Korsmeyer, S.J. Regulators of cell death. *Trends Genet.* **11**, 101–105 (1995).
10. Furuchi, T., Masuko, K., Nishimune, Y., Obinata, M. & Matsui, Y. Inhibition of testicular germ cell apoptosis and differentiation in mice misexpressing Bcl-2 in spermatogonia. *Development* **122**, 1703–1709 (1996).
11. Knudson, C.M., Tung, K.S., Tourtellotte, W.G., Brown, G.A. & Korsmeyer, S.J. Bax-deficient mice with lymphoid hyperplasia and male germ cell death. *Science* **270**, 96–99 (1995).
12. Vergouwen, R.P.F.A., Jacobs, S.G.P.M., Huiskamp, R., Davids, J.A.G. & de Rooij, D.G. Proliferative activity of gonocytes, Sertoli cells and interstitial cells during testicular development in mice. *J. Reprod. Fert.* **93**, 233–243 (1991).
13. Farrow, S.N. *et al.* Cloning of a bcl-2 homologue by interaction with adenovirus E1B 19K. *Nature* **374**, 731–733 (1995).
14. Skinner, M.K. in *The Sertoli cell*. (eds Russell, L.D. & Griswold, M.D.) 237–247 (Cache River Press, Clearwater, Florida, 1993).
15. Xia, Z., Dickens, M., Raingeaud, J., Davis, R.J. & Greenberg, M.E. Opposing effects of ERK and JNK-p38 MAP kinases on apoptosis. *Science* **270**, 1326–1331 (1995).
16. Dudek, H. *et al.* Regulation of neuronal survival by the serine-threonine protein kinase Akt. *Science* **275**, 661–665 (1997).
17. Cailleau, J., Vermeire, S. & Verhoeven, G. Independent control of the production of insulin-like growth factor I and its binding protein by cultured testicular cells. *Mol. Cell. Endocrinol.* **69**, 79–89 (1990).
18. Ayer-LeLiviere, C., Olson, L., Ebendal, T., Hallbrook, F. & Persson, H. Nerve growth factor mRNA and protein in the testis and epididymis of mouse and rat. *Proc. Natl. Acad. Sci. USA* **85**, 2628–2632 (1988).
19. Dirami, G., Ravindranath, N., Kleinman, H.K. & Dym, M. Evidence that basement membrane prevents apoptosis of Sertoli cells in vitro in the absence of known regulators of Sertoli cell function. *Endocrinology* **136**, 4439–4447 (1995).
20. Sharpe, R.M. in *The Sertoli cell* (eds Russell, L.D. & Skinner, M.K.) 391–418 (Cache River Press, Clearwater, Florida, 1993).
21. MacGregor, G.R. & Caskey, C.T. Construction of plasmids that express E. coli beta-galactosidase in mammalian cells. *Nucleic Acids Res.* **17**, 2365 (1989).
22. Ausubel, F.M. *et al. Current Protocols in Molecular Biology*. (Wiley Interscience, New York, 1994).
23. Rowe, L.B. *et al.* Maps from two interspecific backcross DNA panels available as a community genetic mapping resource. *Mamm. Genome* **5**, 253–274 (1994).
24. Chaudhary, J., Cupp, A.S. & Skinner, M.K. Role of basic-helix-loop-helix transcription factors in Sertoli cell differentiation: identification of an E-box response element in the transferrin promoter. *Endocrinology* **138**, 667–675 (1997).
25. MacGregor, G.R., Zambrowicz, B.P. & Soriano, P. Tissue non-specific alkaline phosphatase is expressed in both embryonic and extra-embryonic lineages during mouse embryogenesis but is not required for migration of primordial germ cells. *Development* **121**, 1487–1496 (1995).
26. Sprando, R.L. in *Histopathological Evaluation of the Testis*. (eds Russell, L.D., Ettlin, R.A., Sinha Hikim, A.P. & Clegg, E.D.) 277-280 (Cache River Press, Clearwater, Florida, 1990).
27. Russell, L.D. & Burguet, S. Ultrastructure of Leydig cells as revealed by secondary treatment with a ferrocyanide-osmium mixture. *Tissue Cell.* **9**, 751–766 (1977).